3rd DAAAM International Conference on
Advanced Technologies for Developing Countries ATDC'04
June 23-26, 2004
Split, Croatia

ATDC'04

ANALYTICAL AND EXPERIMENTAL CHARACTERIZATION OF BALL-GROOVE CONTACT PROBLEMS

Saša Zelenika

Abstract

Ball-groove contact problems are often encountered in machine design. The analytical modeling of the resulting stress-strain behavior is however difficult, as it implies the necessity to deal with the non-linear Hertzian theory of point contacts. This work addresses the limits of applicability of the available analytical approaches for the calculation of ball-V groove couplings employed in ultra-high precision positioning. The analytical results are validated experimentally via high-precision measurements.

Keywords: Point Contacts, High-precision Positioning, Experimental Validation

1. Introduction

In the mechanical design of machine elements based on rolling members (e.g. ball bearings, ball screws, …) designers are confronted with the need to consider the behavior of ball-groove contacts, which is difficult to calculate both analytically and numerically. The analysis implies, in fact, the necessity to consider the non-linear Hertz theory of point contacts between elastically deforming solids [1]. In literature, various approaches can be traced which deal with such a problem. The exact model based on the theory of elasticity is complex since it involves an iterative evaluation of elliptic integrals [2]. Other approaches are based on approximated methods making use of diagrams [3, 4], polynomial approximations [5] or interpolating procedures [3, 6, 7] for the calculation of the stress-strain behavior of the bodies in contact as function of the mechanical characteristics and main dimensions of the ball-groove coupling. In high-precision positioning applications, because of the required accuracies in the micrometric and sub-micrometric range, the establishment of the limits of applicability of these approaches is essential.

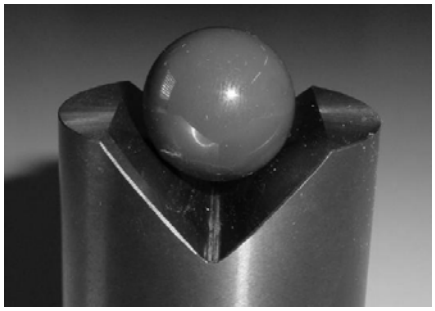

Fig. 1: Ball in a V groove

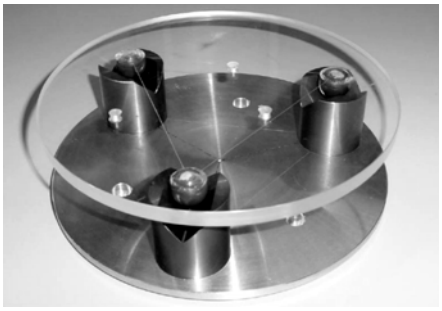

Fig. 2: Kinematic coupling

This work addresses the comparison of the available analytical approaches in the case of a ball-V groove coupling (Fig. 1). The studied configuration is often used in kinematic coupling systems (Fig. 2) employed in ultra-high precision positioning and relocation of opto-mechanical components, in metrology, in scientific apparatuses, by the assembly of micro-parts, in high-precision manufacturing systems and machine tools.

The analytical results obtained for the studied case are then validated experimentally by

employing high-precision measurements. These allow the influence of the various mechanical parameters on the behavior of the ball-V groove contact pairs to be established.

2. Analytical Models

Hertz theory describes the non-linear stress-strain behavior of point contacts between elastically deforming isotropic solids loaded perpendicular to the surface (shear stress, i.e. friction, is neglected), in which the dimension of the contact area is small compared to the radii of curvature and the dimensions of the involved bodies [1-3, 5]. The corresponding exact analytical model entails a lengthy iterative evaluation of transcendental equations involving elliptic integrals (Fig. 3). In fact, by indicating with E_1, ν_1, E_2, and ν_2 the Young's moduli and the Poisson's ratios of the bodies in contact, with F the normal contact load, with R_b the ball radius (R_b=$R_{b\,\min}$=$R_{b\,\max}$) and with $R_{g\,\min}$ the groove radius ($R_{g\,\max}$=∞), the following notation can be introduced [2]:

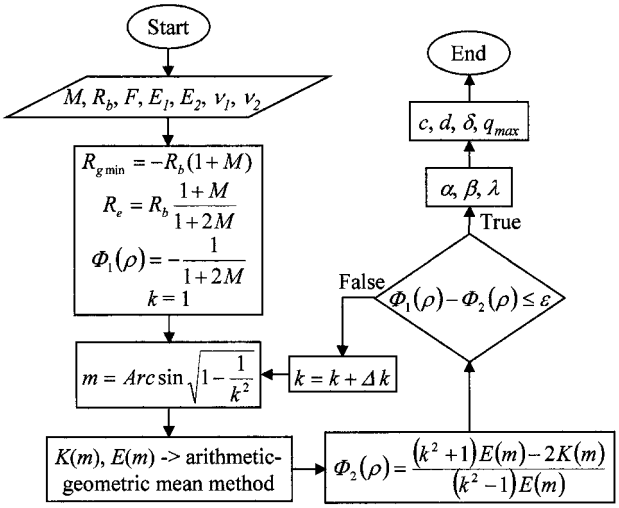

Fig. 3: Exact analytical model

- equivalent Young modulus:

$$E_e = \frac{1}{\frac{1-\nu_1^2}{E_1} + \frac{1-\nu_2^2}{E_2}} \tag{1}$$

- ratio of groove and ball radii of curvature and equivalent radius:

$$M = -\left(\frac{R_{g\,\min}}{R_b} + 1\right) \qquad R_e = R_b \frac{1+M}{1+2M} \tag{2}$$

- curvature difference:

$$\Phi(\rho) = -\frac{1}{1+2M} = \frac{(k^2+1)E(m) - 2K(m)}{(k^2-1)E(m)} \quad (\text{with } \rho = \frac{1}{R_e}) \tag{3}$$

- ratio of the major and minor semi-axes lengths of the elliptical contact area:

$$k = \frac{c}{d} \geq 1 \qquad m = Arc\sin\sqrt{1 - \frac{1}{k^2}} \tag{4}$$

The resulting calculation algorithm is then arranged as shown on Fig. 3, where

$$\alpha = \sqrt[3]{\frac{2k^2 E(m)}{\pi}} \qquad \beta = \sqrt[3]{\frac{2E(m)}{\pi k}} \qquad \lambda = \frac{2K(m)}{\pi}\sqrt[3]{\frac{\pi}{2k^2 E(m)}} \tag{5}$$

are the characteristic parameters, while

$$K(m) = \int_0^{\pi/2} \frac{\mathrm{d}\varphi}{\sqrt{1 - m\sin^2\varphi}} \qquad E(m) = \int_0^{\pi/2} \sqrt{1 - m\sin^2\varphi}\,\mathrm{d}\varphi \tag{6}$$

are the complete elliptic integrals of the first and second kind calculated, as suggested in [8], by employing the arithmetic-geometric mean method.

The results of the algorithm represent the major (c) and minor (d) semi-axes of the elliptical contact area, the interpenetration distance δ of the bodies and the maximum contact stress $q_{\max}$:

$$c = \alpha\sqrt[3]{\frac{3F\,R_e}{2E_e}} \qquad d = \beta\sqrt[3]{\frac{3F\,R_e}{2E_e}} \qquad \delta = \frac{\lambda}{2R_e}\sqrt[3]{\frac{3F\,R_e}{2E_e^2}} \qquad q_{\max} = \frac{3F}{2\pi c\,d} \tag{7}$$

The approximated methods given in literature in which the need to calculate the elliptic integrals is obviated by introducing polynomial [5], tabular [3, 6, 7] or graphical [3, 4] representations of the characteristic parameters are summarized in Table 1 (a is the radius of the circular contact area, α, β, γ, and λ are the characteristic parameters, $\cos\theta$ is dependent on the radii of curvature and ϕ - the angle between the planes of principal curvature; the other parameters are analogous to those given above).

Table 1: Approximated analytical methods

	pol. approx. [5]	interp. [6]	interp. [7]	diagrams [4]	diagrams [3]	gap-bending [5]
R_e	$R_e = R_b \frac{1+M}{1+2M}$	$R_e = 2R_b \frac{1+M}{1+2M}$	$R_e = 1.5R_b \frac{1+M}{1+2M}$	$R_e = R_b \frac{1+M}{1+2M}$	$R_e = 4R_b \frac{1+M}{1+2M}$	$R_e = R_b \frac{1+M}{1+2M}$
$\cos\theta$	$\cos\theta = \frac{R_e}{\lvert R_{g\min}\rvert}$	$\cos\theta = \frac{R_e}{2\lvert R_{g\min}\rvert}$	$\cos\theta = \frac{R_e}{1.5\lvert R_{g\min}\rvert}$	$\cos\theta = \frac{R_e}{\lvert R_{g\min}\rvert}$	$\cos\theta = \frac{R_e}{4\lvert R_{g\min}\rvert}$	/
c	$c = \alpha \sqrt[3]{\frac{3F R_e}{2E_e}}$	$c = \alpha \sqrt[3]{\frac{3F R_e}{4E_e}}$	$c = \alpha \sqrt[3]{\frac{F R_e}{E_e}}$	$c = \alpha \sqrt[3]{\frac{F R_e}{E_e}}$	$c = \alpha \sqrt[3]{\frac{3F R_e}{8E_e}}$	$c = a = \sqrt[3]{\frac{3F R_e}{2E_e}}$
d	$d = \beta \sqrt[3]{\frac{3F R_e}{2E_e}}$	$d = \beta \sqrt[3]{\frac{3F R_e}{4E_e}}$	$d = \beta \sqrt[3]{\frac{F R_e}{E_e}}$	$d = \beta \sqrt[3]{\frac{F R_e}{E_e}}$	$d = \beta \sqrt[3]{\frac{3F R_e}{8E_e}}$	$d = a = \sqrt[3]{\frac{3F R_e}{2E_e}}$
δ	$\delta = \lambda \sqrt[3]{\frac{2F^2}{3R_eE_e^2}}$	/	$\delta = \lambda \sqrt[3]{\frac{F^2}{R_eE_e^2}}$	$\delta = \lambda \sqrt[3]{\frac{F^2}{R_eE_e^2}}$	$\delta = \lambda \sqrt[3]{\frac{9F^2}{64R_eE_e^2}}$	$\delta = \frac{1}{2}\sqrt[3]{\frac{9F^2}{4R_eE_e^2}}$
$q_{\max}$	$q_{\max} = \frac{3F}{2\pi c d}$	$q_{\max} = \frac{3F}{2\pi c d}$	$q_{\max} = \frac{3F}{2\pi c d}$	$q_{\max} = \gamma \sqrt[3]{\frac{F E_e^2}{R_e^2}}$	$q_{\max} = \frac{3F}{2\pi c d}$	$q_{\max} = \frac{a E_e}{\pi R_e}$

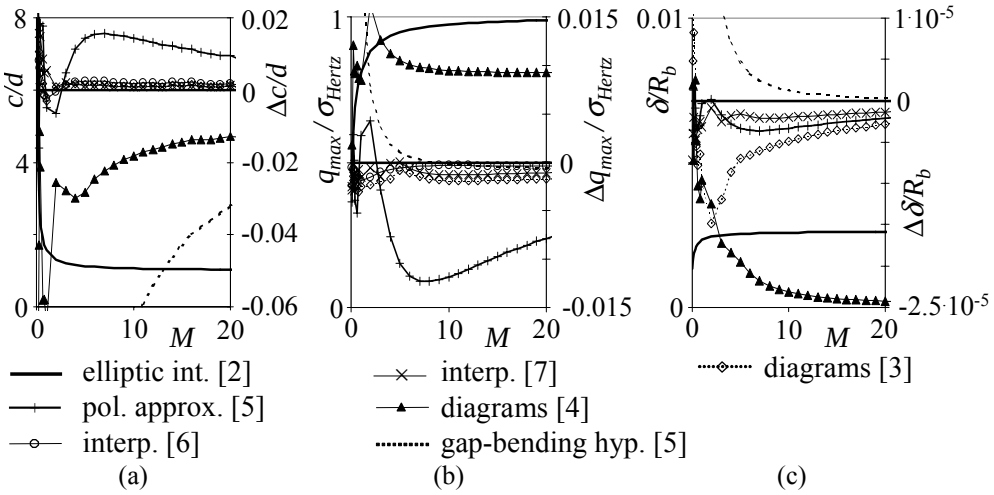

Fig. 4: Ratio of the semi-axes lengths of the elliptical contact area (a), normalized contact stresses (b) and normalized interpenetration distances (c) versus the ratio of the radii of curvature *M*

The analytical results of the ball-V groove contact behavior obtained with the exact approach are compared in Fig. 4 with the approximated analytical methods. For clarity reasons, the results are given as differences of each of the considered method with respect to the exact solution. It can be observed that the gap-bending hypothesis [5], in which the contact between two curved surfaces is reduced to that of a plane and an equivalent sphere, introduces considerable errors. It is worth noticing, however, that this hypothesis yields conservative results, i.e. the calculated stresses and strains are higher than in reality.

The errors introduced by the approximated methods based on polynomial, tabular and graphical representations are always smaller than ±2% (or even, for the methods given in [6, 7], smaller than ±0.2% - Fig. 4). Given the small entity of the stresses and strains involved in most high-precision applications, in absolute terms these errors are negligible in all but those cases in which true nanometric accuracies are sought. Only in the case when the mentioned characteristic parameters approach their limit values (respectively 0 and ∞), which physically corresponds to the

curvature of the groove approaching that of the ball, the errors involved in the approximated methods become appreciable. In this case, however, the basic assumptions of the Hertzian model do not hold any more, and the Hertz theory itself starts to break down [5].

3. Experimental Assessment

In high-precision applications the repeatability of the couplings has to be addressed [5]. The considered analytical approaches cannot, however, take into account the extent of non-repeatability caused by friction, as this effect can be evaluated only with elaborated numerical formulations based on incremental variational inequalities [9]. Even in that case, however, the extent of variation due to the stochastic nature of friction is not taken into account. Moreover, since the magnitude of the deflections is often in the sub-micron range, surface finish plays an important role. In fact, real solids make contact only where the asperities on the two surfaces come together, and Hertzian analysis is thus merely the limit case to which real contacts tend [10]. Other effects (e.g. load asymmetry) also affect repeatability.

In order to examine thus the repeatability and, as the most important feature in high-precision applications, the interpenetration distance of the ball-V groove contacts, an experimental set-up was built (Fig. 5). Gothic-arch shaped grooves ($R_{g\,\min}$=12mm÷∞) with polished contact surfaces (R_a=100nm) are built as modular inserts and epoxied onto the lower plate. In order to make the compliance of balls' fixation low compared to that of the coupling, the balls (R_b=5.5÷10 mm, R_a=20÷60nm) are inserted into conical seats in the upper plate, burnished until the surface is brinelled, and then epoxied [5]. The set-up is thermally isolated (a stability of ±0.1°C was reached). Stainless steel grooves and balls of various hardness (HRC 34÷67) are used. To minimize fretting corrosion, friction, as well as the footprint (i.e. to approach as much as possible true point contacts) [5], ceramic (tungsten carbide (WC) and silicon nitride (Si_3N_4)) grooves and balls are also employed. The loads are applied to the coupling via a pneumatic piston, and their magnitudes are measured with a precision (±0.25% ES) calibrated load cell. The interpenetration distance is measured with linear absolute encoders (HEIDENHAIN type CT 6002, resolution: 5nm, accuracy: ±100nm). Two encoders are used to have control of the symmetry of the behavior.

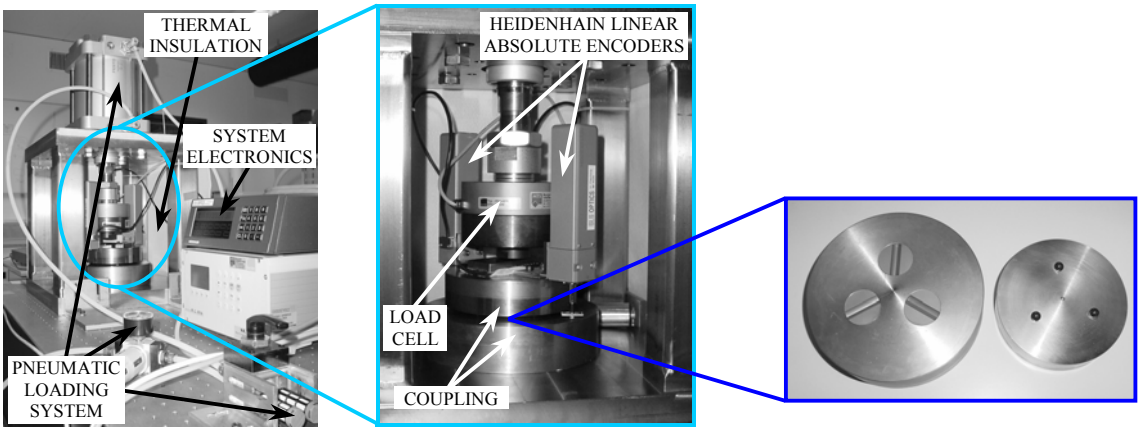

Fig. 5: Experimental set-up (a) with detail of the load and displacement measurement systems (b) and of the coupling elements (c)

The results of cyclic measurements (25 cycle averages with 100 points in each cycle) and the corresponding theoretical data calculated by using the exact analytical model are shown in Fig. 6. The interval of uncertainty (up to ±10% of the measured values) is mainly due to dimensional tolerances of the couplings' components, the residual compliance (e.g. epoxied connections) and the uncertainty in the mechanical properties of the used materials (cf. [6]). Despite the care devoted to the set-up of the experimental apparatus, this uncertainty is hence much larger than the errors introduced by adopting the considered approximated analytical methods. The obtained results can be summarized as:

- In all the considered cases, the theoretical values of the interpenetration distance are within

the intervals of uncertainty of the measurements, regardless of the used materials.

- For small loads the measured values are smaller than the theoretical ones, which could be due to surface roughness and the resulting flattening of the contact points ("micro-approaching" [2]). This is supported also by the observed brinelling of contact surfaces (Fig. 7). Previous studies have allowed establishing that, because of surface roughness, for light loads the peak pressure can be up to 70% smaller and the contact area up to 10 times larger than in theory [10]. Moreover, the micro- and nano-hardness and Young's moduli differ from the macroscopic ones and depend on the state of the surface, which can have a significant impact on the results in this region, too.
- For higher loads the experimental results are closer to the theoretical ones, which could be due to the lower influence of the surface finish and the residual compliances in this region. By using ceramic coupling components, a tendency towards higher measured interpenetration distances than those calculated theoretically was observed. This could be due to the uncertainty of the mechanical properties of ceramic materials.
- Although lubrication generally has a small effect (Fig. 6), in some instances it induces a lowering of the measured values (≤ 10%). The explanation for this event was not found.
- After a wear-in period of less than 50 cycles, the repeatability of the couplings is typically in the $\sigma \leq 100$ nm range (comparable to the surface finish of the coupling interface). The residual non-repeatability could be due not only to surface finish, but also to non-linearities such as creeping or pre-sliding displacement.

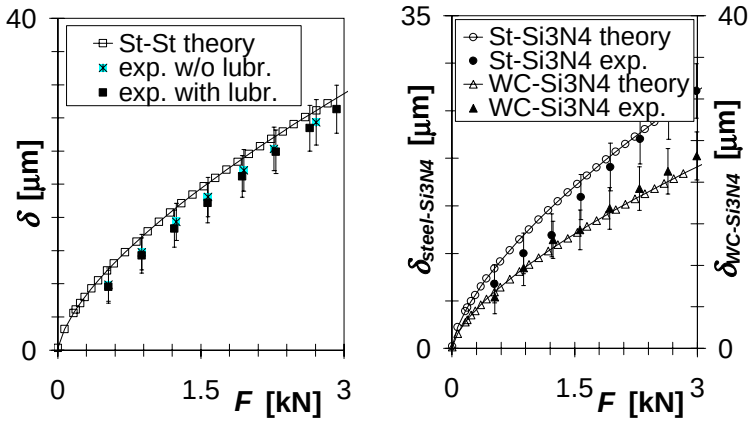

Fig. 6: Comparison of theoretical and experimental results for different materials

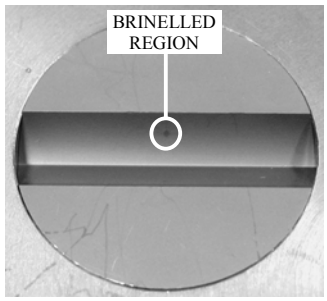

Fig. 7: Brinelling of the contact surface

A trial was also performed to measure the area of the contact region by optical means, i.e. by employing a 3D ZYGO type Newview 5010 scanning white-light interferometry-based surface profiler used to characterize the polishing accuracy of optical surfaces (vertical resolution: 0.1nm, RMS repeatability: 0.4nm, lateral resolution: 4.72µm). It was hence shown that:

- In the elastic domain the results are characterized by low accuracy (Fig. 8) and big dispersion.

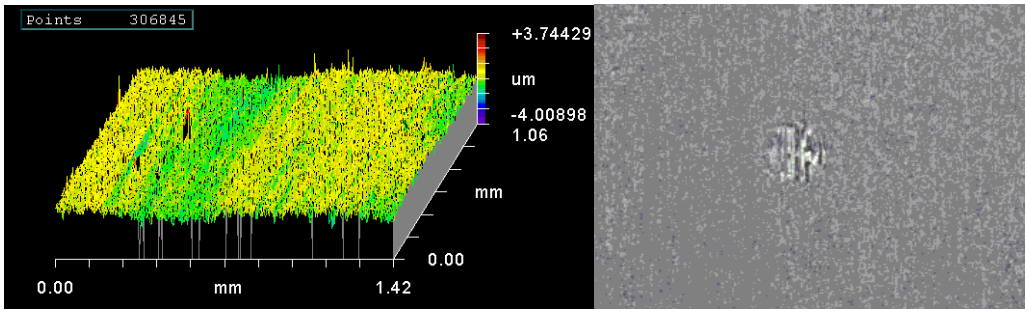

Fig. 8: Interferometric measurement of the contact area in the elastic domain

- In the plastic domain a good accuracy is obtained (Fig. 9) but the results are of little practical

use (all the cited theoretical approaches are valid only in the elastic domain).

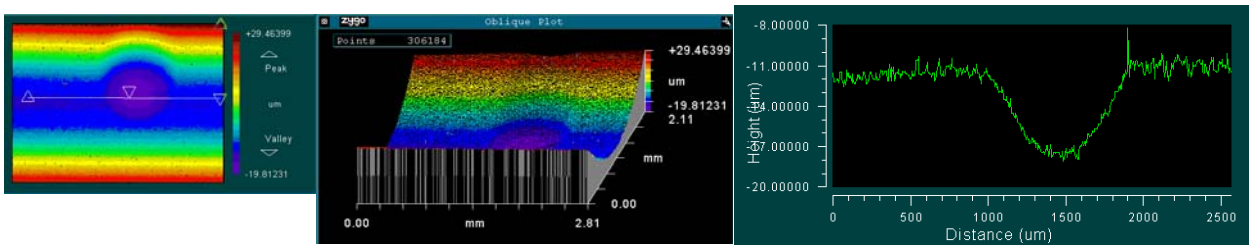

Fig. 9: Interferometric measurement of the contact area in the plastic domain

- Previous trials to measure the contact area by using contact resistance measurements or photo-elasticity have also given results characterized by low accuracy. Perhaps only the usage of newly developed pressure sensitive films (cf. www.sensorprod.com) could allow the situation in this regard to be improved.

4. Conclusions

Except for the gap–bending hypothesis method, the approximated analytical approaches available in literature for the evaluation of the stress-strain behavior of ball-V groove contact problems are giving results equivalent to those obtained with the exact analytical model in the micrometric and sub-micrometric domain, and are therefore of suitable accuracy for most of the practical cases encountered in dimensioning high-precision couplings.

In the whole range of elastic deformations, the correspondence of the theoretical values of the interpenetration distances with the experimental ones is within the intervals of uncertainty of the latter, regardless of the used materials and lubrication conditions. These effects seem, in fact, to influence the behavior only in the sub-micrometric range.

The repeatability of the couplings is comparable to the surface finish of the contact interface and thus it is in the 100 nm range.

Despite the high accuracy of the employed measurement technique, the measurements of the contact area are characterized by low accuracy and are left to eventual future studies.

Acknowledgement

A special thank is due to S. Flechsig, without whom the presented results would not have been obtained.

References

[1] Hertz, H., “Gesammelte Werke - Band I”, J. Ambrosius Barth, Leipzig D, 1895.
[2] Harris, T.A., “Rolling Bearing Analysis” – 3rd ed., John Wiley, New York USA, 1991.
[3] Jacazio, G., and Piombo, B., “Meccanica applicata alle machine”, Levrotto & Bella, Torino I.
[4] Jacazio, G., “Progettazione delle strutture meccaniche”, Eda, Torino I, 1985.
[5] Slocum, A.H., “Precision Machine Design”, Prentice Hall, New Jersey USA, 1992.
[6] Timoshenko, S.P., and Goodier, J.N., “Theory of Elasticity”, McGraw Hill, New York USA, 1970.
[7] Young, W.C., “Roark’s Formulas for Stress and Strain”, McGraw-Hill, New York USA, 1989.
[8] De Bona, F., and Zelenika, S., "A generalized Elastica-type approach to the analysis of large displacements of spring-strips", J. Mech. Eng. Sci. – Proc. Ins. Mech. Eng. C, Vol. 211, 1997, pp. 509-517.
[9] Li, M., et al., “Linear Complementary Formulations Involving Frictional Contact for Elasto-Plastic Deformable Bodies”, J. Appl. Mech. - ASME, Vol. 64, 1997, pp. 80-89.
[10] Greenwood, J.A., and Tripp, J.H., “The Elastic Contact of Rough Spheres”, J. Appl. Mech. - ASME, 1967, pp. 153-159.

Dr. sc. Saša Zelenika, Assistant Professor
University of Rijeka, Faculty of Engineering, Vukovarska 58, 51000 Rijeka, Croatia, Sasa.Zelenika@riteh.hr and Paul Scherrer Institut – Head of Division of Mechanical Engineering Sciences, 5232 Villigen PSI, Switzerland, telephone: + 41 - (0)56 – 3104586; fax: + 41 - (0)56 – 3102549; e-mail: sasa.zelenika@psi.chT